Applied Surface Science 481 (2019) 1490–1502

Contents lists available at ScienceDirect

Applied Surface Science

journal homepage: www.elsevier.com/locate/apsusc

Full length article

Ex-situ SIMS characterization of plasma-deposited polystyrene near atmospheric pressure

Vanina Cristaudo[a,*], Delphine Merche[b], Claude Poleunis[a], Jacques Devaux[a], Pierre Eloy[a], François Reniers[b], Arnaud Delcorte[a]

[a] Institut de la Matière Condensée et des Nanosciences (IMCN), Bio & Soft Matter (BSMA), Université catholique de Louvain (UCL), 1 Place Louis Pasteur box L4.01.10, B-1348 Louvain-la-Neuve, Belgium

[b] Chimie Analytique et Chimie des Interfaces (CHANI), CP 255, Université Libre de Bruxelles (ULB), 2 Boulevard du Triomphe, B-1050 Brussels, Belgium

ARTICLE INFO

Keywords:
Plasma polymerization
Dielectric barrier discharge
ToF-SIMS
Organic depth-profiling
Surface contamination
Oxidation

ABSTRACT

Polystyrene-like coatings are synthesized by plasma near atmospheric pressure. Elucidating their chemical structure after exposure to ambient air could be very challenging because of the interference of surface-related phenomena, mainly post-polymerization oxidation and contamination. In this paper, we propose secondary ion mass spectrometry (SIMS) in molecular depth-profiling mode, combined to multivariate analysis, as a more reliable tool for their investigation as a function of the injected power. Indeed, the information provided by the inner layers is more representative of the film in growth. The SIMS approach is validated by complementary, surface-sensitive and bulk techniques: X-rays photoelectron spectroscopy (XPS) and infrared spectroscopy (IR). The SIMS results suggest that the high concentration of -CH_3 groups in the polymer matrix, pointed out by IR, is due to branching and/or grafting of CH_3· radicals to active sites (prevalently in position α, β, γ) along the aliphatic backbone, in addition to a significant fraction of trapped oligomers. The oligomer contribution is supported by an original study based on the molecular weight dependence of the sputtering efficiency. The overall experimental evidences indicate a milder fragmentation of the precursor at lower powers, leading to a higher conservation of the aromaticity and a lesser branched and/or cross-linked content.

1. Introduction

Plasma-polymerized polystyrene (pp-PS) is mainly used as a protective film and in the preparation of medical and electronic devices. A considerable amount of research has been conducted on the plasma polymerization of the styrene precursor at low pressure since the 1960s [1–6], but to our best knowledge only a few works have addressed the more recent use of atmospheric pressure devices [7–9]. The advantages of using plasma technologies for the deposition of polymer-based materials at atmospheric pressure are presented in a review paper [10]. Consequently, the elucidation of the chemical structure of pp-PS obtained near atmospheric pressure is desired by the scientific community.

Well-established protocols for the characterization of plasma-deposited polymers include complementary surface-sensitive and bulk techniques, such as X-ray photoelectron and infrared spectroscopies [11–13]. In this context, secondary ion mass spectrometry (SIMS) is still considered as a more exotic technique. This is probably due to the extensive fragmentation of the polymer chains upon primary ion bombardment (of a few tens of keV), so that the extraction of chemical and structural features from the SIMS spectra (i.e. static-SIMS or SSIMS mode) is not straightforward and sometimes extremely time-consuming. However, the potential of SSIMS as a surface characterization technique for the direct interrogation of plasma-deposited and plasma-treated polymer structures was pointed out a long time ago, when the mass resolution was still strongly limited by the use of quadrupole mass analyzers [14,15]. Chemical and structural information provided by SIMS is unique and extremely valuable for the analysis of plasma-related polymers (treated or synthesized by plasma), providing insights about the unsaturation, branching and/or cross-linking contents. An example is given by the SIMS study of plasma-induced surface modifications of polymers conducted by De Puydt et al. in 1992 [16]. In their work, information about the unsaturation and cross-linking was retrieved by means of SIMS structural indicators [17], such as the sum

* Corresponding author.
E-mail addresses: vanina.cristaudo@uclouvain.be (V. Cristaudo), Delphine.Merche@ulb.ac.be (D. Merche), claude.poleunis@uclouvain.be (C. Poleunis), jacques.devaux@uclouvain.be (J. Devaux), pierre.eloy@uclouvain.be (P. Eloy), Francois.Reniers@ulb.ac.be (F. Reniers), arnaud.delcorte@uclouvain.be (A. Delcorte).

https://doi.org/10.1016/j.apsusc.2019.03.032
Received 8 November 2018; Received in revised form 27 February 2019; Accepted 2 March 2019
Available online 21 March 2019
0169-4332/

of the aromatic ion intensities (Σarom) [18]. In 1994, Petrat et al. carried out a combined SSIMS and XPS in-situ analysis to study the surface modifications of PS induced by Ar, O_2 and N_2 microwave plasmas [19]. The destruction of the aromaticity was pointed out by the $C_7H_7^+/C_4H_7^+$ signal ratio in SIMS and supported by the ratio of aromatic to aliphatic carbon in the XPS C 1s signal. In 1995, plasma-polymerized styrene thin films were studied with SIMS and XPS by Leggett et al. They found out that SSIMS analysis was very sensitive to the cross-linked and unsaturated contents on the basis of a structural comparison between conventional and plasma-polymerized PS [20]. Furthermore, the effects of the external plasma parameters on the chemical structure of plasma-deposited polymers have been widely investigated by time-of-flight (ToF)-SIMS surface analysis [21]. High functional group retention and structural retention from the precursors were achieved in the plasma polymerization at low power and high precursor flow rate. This was frequently observed in the SIMS surface characterization of plasma-polymers [22,23]. A ToF-SIMS investigation of the chemical character of plasma-deposited films from ethylene and styrene at low pressure and as a function of the external plasma parameters was conducted by Oran et al. [24]. Additional SIMS structural indicators were employed in the surface characterization of plasma-synthesized films from the styrene, allyl alcohol, and allylamine precursors, which were also correlated to the different deposition conditions [25]. In general, harder plasma conditions, such as higher power or lower precursor flow rate, result in higher irregularity of the plasma films (because of a decreased retention of the precursor functionalities and/or higher cross-linked/branched/unsaturated contents). Studies also indicated that the lower the irregularity of the film, the higher was the post-oxidation and vice versa [26]. More recently, multivariate analysis was applied in the SSIMS studies of plasma-treated and plasma-synthesized polymers in order to readily extract a higher amount of chemical and/or structural information based on the interpretation of the most important variation trends of the ToF-SIMS ion intensities. The potentialities of combining SSIMS and multivariate analysis for the characterization of ultra-thin plasma films are well demonstrated by a recent publication of Cossement et al. [27]. It reviews the work conducted by their group in Mons on the characterization of plasma-polymers in order to extract the relative cross-linking degree [28–33].

In this paper, polystyrene-like films were deposited by means of a dielectric barrier discharge (DBD) and the plasma power was varied between 10 and 80 W. The coatings were then analyzed ex-situ. In contrast to the extensive literature on static-SIMS characterization of plasma-polymer surfaces which is adequate for in-situ analysis, one novelty of the present study is that it investigates the sub-surface, being more representative of the actual chemical structure after exposure to air [34]. This is made possible thanks to the recent advent of massive Ar cluster ion beams as “damageless” sputtering sources for organic materials [35]. However, one is dealing with a polymer showing new structural features not ascribable to the conventionally polymerized counterparts (chosen as references in this work) for which, as was mentioned above, traditional structural indicators have been defined in SIMS [20]. Hence, multivariate analysis was chosen in order to extract more reliable information about the pp-PS structure from the mass spectra [36]. Specific chemical and structural features of the pp-PS deposits, such as methyl-substitution and oxidation, were elucidated by SIMS. In the end, the integration of the information derived from gel permeation chromatography (GPC), XPS (surface-related), IR and SIMS/PCA (bulk-related) lead to a more complete picture of the chemical structure of the investigated plasma-polymer, as well as its dependence on the power injected into the plasma medium.

2. Experimental section

2.1. Materials

The liquid styrene precursor used for the plasma polymerization was provided by Fluka (99.5% purity, 0.005% of 4-*tert*-butylcatechol as stabilizer). The styrene was employed without any further purification. Argon was chosen as carrier gas and plasmagen gas (Air Liquide, 99.999% purity). The plasma-polymerized styrene was deposited onto silicon substrates of $1 \times 4–5\ cm^2$ size, cleaned by sonication in isopropanol (VWR Chemicals, HiPerSolv CHROMANOFORM for HPLC, 99.9% purity) and dried under nitrogen flux. Each $1 \times 4–5\ cm^2$ Si-supported plasma film was successively cut in $1 \times 1\ cm^2$ pieces to be characterized by the different analytical techniques. This methodology was found to be the best in order to avoid the edge effects and to obtain more homogeneous films in terms of chemical structure and thickness. Linear and cross-linked PS, used as reference samples, was purchased from Goodfellow (~1 mm-thick polymer sheets). Other commercial references were employed in the SIMS study, such as the poly (α-methyl styrene) (PAMS), poly (4-methyl styrene) (P4MS) and poly (4-vinylphenol) (PVP). Polydisperse PAMS was provided by Scientific Polymer Product. P4MS (M_w ~72,000 g/mol) and PVP (M_w ~25,000 g/mol) were purchased from Sigma-Aldrich. In order to prepare Si-supported thin films, first PAMS and P4MS powders were dissolved in toluene (Sigma-Aldrich, purity ≥99.71%), whereas PVP was dissolved in isopropanol (VWR Chemicals, 99.9% purity). Then, the solutions were spin-coated onto the cleaned silicon at 5000 rpm with acceleration 20,000 rpm/s for 60 s.

2.2. Plasma polymerization

Plasmas were produced in a homemade dielectric barrier discharge (DBD) reactor (scheme in supporting information, Fig. S1). The reactor consists in a glass cylinder made of pyrex from PierreGlass, 7-mm thickness, 200-mm height and 100.5-mm radius with six entries (KF DN 25) located at half-height for the gas inlets and the pressure gauge. It is connected to two UHV stainless-steel flanges (SA Georis) and the insulation is ensured by two Viton O-rings. Each UHV stainless-steel flange presents two feedthroughs KF DN 16 for the passage of current (on the top) and the pumping system (on the bottom). The remaining unused feedthroughs are closed with OD flanges. Two copper electrodes, covered with aluminum oxide (alumina, 99.7% purity), with 8-cm diameter and 3-mm thick are provided by Ceratech. The inter-electrodes distance is 3–4 mm. High voltage is applied to the top electrode, whereas the bottom electrode is grounded. The DBD device is equipped with two different gas inputs: 1) mixture of carrier gas and styrene (precursor), and 2) only carrier gas, that in this case is employed to bring the chamber to atmospheric pressure. The liquid styrene precursor is kept at 313 K in a bubbler immersed in a thermostated bath. The precursor vapors are carried into the discharge by an Ar flux via a volumetric flowmeter from Aalborg with a flow rate of 4 L/min. The gases are driven to the plasma chamber using PFA (perfluoroalkoxy copolymer) and stainless-steel lines (Swagelok®). The lines are heated by thermal bands from the bubbler to the chamber in order to minimize the precursor condensation. After the introduction of the silicon substrate for the plasma deposition on the bottom electrode and perpendicularly to the Ar/styrene inlet, the chamber is pumped down to a pressure of $1 \times 10^2–5 \times 10^2$ Pa by a primary pump “Chemvac combination pump system 6 Dp-101”. Then, the chamber is refilled by the gas mixture (Ar/styrene) to the working pressure of 2×10^4 Pa measured by a gauge CMR 361. The cylindrical chamber is pumped continuously during the plasma polymerization (dynamic flux) in order to minimize the air contamination of the growing polymer film. A dosing valve Balzers-Pfeiffer Vacuum EVN 116 is located between the pump and the chamber in order to reduce the pumping rate during the film deposition. The low frequency (LF) plasma is ignited using an AFS (G10 S-V) generator. The frequency is fixed at 18,160 Hz. Plasma-polymer films were prepared varying the power from 10 W to 80 W. The deposition time was kept constant at 5 min. After the film deposition, the sample was left in the reactor under (sub)-atmospheric pressure during 5 additional minutes in order to minimize the post-

Table 1
List of the investigated plasma-deposited styrene films polymerized at different powers and commercial PS samples used as references. Note that the linear PS represents the main reference material for the XPS, IR and SIMS analyses.

Plasma-polymerized polystyrene (pp-PS) films		
Plasma power (W)	Sample name	Film thickness (μm)[a]
10	pp-PS/10W	0.13
20	pp-PS/20W	0.57
30	pp-PS/30W	1.77
40	pp-PS/40W	1.60
50	pp-PS/50W	4.14
60	pp-PS/60W	6.03
70	pp-PS/70W	8.18
80	pp-PS/80W	4.71

Polystyrene and derivatives (references)	
Polymer	Chemical structure
Linear PS	
Poly (α-methyl styrene), PAMS	
Poly (4-methyl styrene), P4MS	
Poly (4-vinylphenol), PVP	
Cross-linked PS	–

[a] Estimated by stylus profilometry in the center of 1 × 1 cm^2 samples.

polymerization oxidation due to the surviving radicals trapped inside the polymer structure. Then, the plasma chamber was brought to atmospheric pressure with argon and the samples were collected to be analyzed. The plasma-synthesized films do not appear oily and sticky in contrast with the deposits obtained in other works at high pressures or low power levels [3,23], suggesting that they are cross-linked to a certain extent. The samples investigated in this study and the reference polymers are described in Table 1.

2.3. Characterization of the samples

2.3.1. ToF-SIMS in-depth analysis and PCA data treatment

SIMS molecular depth-profiling experiments were performed using an ION-TOF TOF.SIMS 5 (Münster, Germany) instrument equipped with both Bi(Mn) Nanoprobe-LMIG (liquid metal ion gun) and Ar-GCIB (gas cluster ion beam) primary ion sources mounted at 45° to the surface normal. The secondary ions were collected by a reflectron-type time-of-flight analyzer perpendicular to the sample surface. The plasma-polymer samples were analyzed ex-situ by SIMS within the first few hours from their preparation. The molecular depth-profiles were acquired only in positive ion polarity, due to the poor hydrogen-related information provided by the negative ion polarity. However, important insights about the oxidation can also be extracted from the positive ion mode. The depth-profiling was performed in non-interlaced dual ion beam mode. So, a 10-keV Ar_{3000}^+ ion beam was employed to sputter a 600 × 600 μm^2 area, whereas a second pulsed beam of 30-keV Bi_5^+ ions (0.06 pA) was used to collect the mass spectra from a 200 × 200 μm^2 area, concentric to the sputtered surface. The sputter current was set to 2 nA for all the experiments with the exception of the thinnest plasma films (10 W and 20 W), where it had to be lowered to 0.3 nA. A 20 eV electron flood gun was employed for charge compensation. The mass resolving power at m/z 29 ($C_2H_5^+$) was around 5000 which is sufficient to resolve the hydrocarbon from the O-containing peaks in the low mass region. For the thickest plasma-deposited films (from 30 to 80 W), the total ion dose cumulated over an entire profile for the 30-keV Bi_5^+ beam was of the order of 10^{12} ions/cm^2, while for the 10-keV Ar_{3000}^+ source it was kept around 5 × 10^{14} ions/cm^2. The ratio between the analysis and sputter doses excludes a significant contribution of the Bi_5^+ beam in the etching process of the specimens [37,38]. In the above-mentioned sputter conditions, sputtered volumes of ~250 nm and ~190 nm in depth were measured for the pp-PS/40W and pp-PS/80W specimens, respectively. The sputtered depths were measured by a stylus profilometer DektakXT (Bruker Nano Surfaces Division, Tucson AZ, USA) in 3D imaging mode with a 0.7-μm tip and applying a force of 0.3 mg in order to estimate the sputter yield volume Y (expressed in nm^3/primary ion or nm^3/PI) of the polymer materials. Y was calculated by dividing the sputtered depth (nm) by the sputter ion dose (PI/nm^2) needed.

The bulk-like mass spectra used in this study were obtained by means of a computer reconstruction of the SIMS raw data over a sputter dose of ~4 × 10^{13} ions/cm^2, ~3 × 10^{14} ions/cm^2, ~7 × 10^{14} ions/cm^2 for the pp-PS films polymerized at 10–20 W and 30–80 W, and the commercial linear PS, respectively. These depth-regions of the profiles show high stability of the most characteristic fragments of the PS (like for instance $C_7H_7^+$, $C_8H_9^+$ and $C_9H_9^+$) and some O-based ions observed in the pp-PS deposits (such as CH_3O^+ and $C_2H_3O^+$). Principal component analysis of the bulk-like positive ion mass spectra was conducted using the Spectragui code developed by NESAC/BIO (http://www.nb.uw.edu/). In order to perform the multivariate analysis, three molecular depth-profiles were acquired per sample, because of the high homogeneity of the plasma films. A manual selection and integration of the peaks was made in the m/z range 12–210 of ~170 hydrocarbon and ~70 O-containing secondary ions (since the pp-PS is oxidized). This m/z range covers most of the "fingerprint region" of the mass spectrum, where the fragmentations of the PS repeat unit -(C_8H_8)- (repeat unit M_w = 104.1 g/mol) and the bigger moieties -$(C_8H_8)_n$- (with n = 2, 3, …) overlap. This m/z region represents a large fraction of the total intensity of the mass spectrum, permitting to extract a large amount of structural information about the polymer (e.g. aromaticity, branching and cross-linking). When additional polymer references were included in the PCA models (PAMS, P4MS, PVP, cross-linked PS), the previous peak list was adjusted to the new set of samples, including 283 ion contributions. Before multivariate analysis, the data set was normalized and mean-centered. The normalization to the total intensity of the reconstructed mass spectrum was performed in order to eliminate the variance produced by a systematic error due to the variation of the secondary ion formation efficiency, which depends on matrix effect, surface topography, charging effects and instrumental factors. The mean centering procedure ensures that the observed differences in samples were due to variations around the means and not to the variance of the means. The explanation of the PCA method is reported elsewhere [36].

2.3.2. XPS analysis

XPS spectra were acquired using a Kratos Axis Ultra spectrometer (Kratos Analytical, Manchester, UK) equipped with a monochromatized aluminum X-ray source (powered at 10 mA and 15 kV). The pressure in the analysis chamber was about 10^{-6} Pa. The angle between the normal to the sample surface and the direction of photoelectrons collection was 0°. The pass energy was set to 160 eV for the survey scan and 40 eV for narrow scans (C 1s, O 1s and Si 2p). The $\underline{C}_{aliph}$-(C,H) component of the C 1s peak of carbon was fixed at 284.8 eV to set the binding energy scale [39]. The decomposition of the C 1s peak in its oxidized components was performed by fixing the following binding energies, allowing to reliably comparing the different samples (Fig. S2): 288.8 eV for COOR/COOH (indicated as O=$\underline{C}$-O), 287.8 eV for RR'C=O ($\underline{C}$=O, O-$\underline{C}$-O) and 286.3 eV for C-OR/C-OH ($\underline{C}$-O). Molar fractions (%) were calculated using peak areas normalized on the basis of the acquisition parameters after a linear background subtraction, the experimental sensitivity factors (C = 0.278, O = 0.780 and Si = 0.328 based on those of

Wagner) [40] and the transmission factors provided by the manufacturer. The XPS analyses were conducted on the same plasma samples used for SIMS, immediately after the depth-profiling experiments.

2.3.3. FT-IR analysis

FT-IR spectra of pp-PS films were recorded on a Nicolet spectrometer (Nexus 870), equipped with Continuum microscope, in transmission mode. FT-IR spectra were obtained with 32 scans at a resolution of 8 cm^{-1} over a spectral range from 4000 to 500 cm^{-1}. The samples pp-PS/10W and pp-PS/20W were too thin for the IR analysis (cf. Table 1). On the contrary, as they were too thick, IR spectra of the two commercial polymer sheets, linear and cross-linked PS, were performed with the same apparatus in ATR (attenuated total reflectance) mode, using a silicon crystal in mono-reflection. A total of 128 scans were taken with a resolution of 8 cm^{-1} over a spectral range from 4000 to 650 cm^{-1}. Baselines were corrected manually. Qualitative information was essentially extracted from the IR analyses because of the absence of an internal reference for the normalization of the spectra, in addition to the uncertainty of the film thickness that varies strongly both in x and y directions.

2.3.4. GPC analysis

Only two pp-PS films deposited at different plasma powers were selected for the GPC characterization, i.e. pp-PS/30W and pp-PS/60W. Each polymer film on a Si substrate was immersed in toluene (Sigma-Aldrich, purity ≥99.71%) for 16 h and heated at 40 °C to favor the dissolution. Then, the silicon substrate was removed from the solvent, even if the wafer was still covered by a polymer deposit. The solution was concentrated, then dried. A new solution was prepared in dimethylformamide (DMF) with a concentration of 1–2 mg/mL. The solution was filtered prior the GPC analysis with a 0.2-µm Teflon filter in order to remove any undissolved (pp-PS, dust…) particles. Molecular weights (M_w) of the polymers were measured on an Agilent gel permeation chromatography system equipped with an Agilent 1100/1200 pump (35 °C, eluent: DMF; flow rate of 1 mL/min), an Agilent differential refractometer and two PSS GRAM columns (beads 10 µm; porosity of column 1: 1000 Å; porosity of column 2: 100 Å). The calibration was performed using polystyrene standards.

3. Results

The protocol established in this paper for the ex-situ characterization of the pp-PS films as a function of the discharge power is depicted in Scheme 1. It can be described as follows:

1) The elemental composition and the chemical bonds at the samples' surface were first elucidated by XPS (sampling depth is ~10 nm) and compared with the conventionally polymerized counterpart, i.e. linear PS. This analysis is strongly influenced by adventitious contamination and other surface-related phenomena;
2) Plasma-polymer films were also analyzed in the bulk by FT-IR (sampled depth of several µm), bringing information about the C-H_x bonds and O-based functional groups;
3) GPC analysis was carried out in order to verify the size distribution of the soluble fraction of the plasma-polymer chains. Additionally, the Ar cluster sputtering efficiency in SIMS was estimated for the pp-PS films, providing important insights about the presence of oligomers trapped in the polymer matrix;
4) Main characterization of the pp-PS films was conducted by ToF-SIMS in the inner layers of the specimens via:
   a) Acquisition of depth-profiles in positive ion polarity (+) by large Ar cluster bombardment and identification of the steady state region of the characteristic structure-related fragments where most of the phenomena occurring near the surface can be safely discarded, such as air contamination [41], post-polymerization oxidation [24,26], segregation of low molecular weight chains, inhibitors of the utilized precursor towards the surface (and additives present in the conventionally synthesized PS references) [41], and chains re-orientation at the air/polymer interface;
   b) Reconstruction of the "bulk-like" mass spectra in the sub-surface region of the plasma-deposited films (along several hundreds of nm), in which the chemical structure appears to be homogeneous;
   c) Application of multivariate analysis (PCA) and its interpretation.

The proposed approach allows the SIMS, typically known as a surface-sensitive technique (sampled depth of ~3 nm), to be compared with bulk analytical techniques like IR spectroscopy. In the Discussion section, it will be shown how the IR results (and XPS) help to confirm the complex picture of the pp-PS chemical structure drawn from the SIMS bulk analysis.

3.1. XPS surface characterization

The surface elemental composition of the reference sample - linear PS - and the pp-PS films deposited at plasma powers ranging from 10 W to 80 W is reported in Table 2. The XPS characterization of the commercial "linear PS" confirms that, in terms of purity, the chosen material is a good reference for this study. Indeed, it consists of 99.3% of carbon and only 0.7% of oxygen, explainable by surface contamination. The percentage of the shake-up satellite, ascribed to π-π^* transitions of the aromatic rings of PS and unsaturated side chains, is very close to the one reported in the XPS library (~10% of $\underline{C}_{arom}$-(C,H)) [39]. On the other hand, the pp-PS films differ fundamentally from the PS reference by the much higher content in O ranging from ~7% to ~9%. Surface contamination could be inferred from the detection of the Si 2p peak, which does not come from the substrate because it is uniformly covered by the plasma film. The O-uptake of the plasma-polymers could take place during the plasma polymerization and/or be due to post-polymerization oxidation in the air, since radical species remain trapped in the film after plasma deposition [42]. A correlation between the $\underline{C}$-O component of the main C 1s peak and the O 1s peak is also found, so that the O-uptake in all these polymer structures mostly occurs via C-O simple bonds. For the pp-PS films, the O 1s/$\underline{C}$-O ratio indicated in the last column of Table 2 is close to 1, suggesting the preponderant presence of alcohol functionalities (C-OH) independently of the power applied during the plasma deposition. Additionally, the O content of the pp-PS increases slightly with power (cf. the O 1s column of Table 2). This variation is significant considering that repeated measurements on selected plasma samples (up to four XPS spectra) highlighted a high homogeneity of the pp-PS surfaces (± 0.2% standard deviation for 10 W). This increase in oxidation going from 10 W to 80 W seems to occur at the expense of the aromaticity, as pointed out by the decrease of the shake-up satellite (~1%). This could suggest an oxidative functionalization of the phenyl rings with subsequent disruption of the aromaticity [42].

3.2. FT-IR bulk characterization

The IR-ATR spectrum of the linear PS (reference) depicted in Fig. 1.a shows the main finger-printing IR bands of the polystyrene [3,12]. The IR assignments of the main characteristic bands of PS are reported in Table S1. In particular, both bands of the mono-substituted aromatic ring at 756 cm^{-1} and 701 cm^{-1} are unequivocally identified, as well as the so-called "five aromatic finger" (overtone) bands between 1943 and 1666 cm^{-1}. They are assigned to the out-of-plane bending deformation ω of the mono-substituted aromatic ring. Thus, these overtones tend to disappear in PS derivatives like P4MS (para-substituted), chosen as additional reference for the SIMS analysis [25]. Furthermore, the bands at 1600, 1580, 1492 and 1450 cm^{-1} appear in the IR spectrum, due to the vibration ν of the aromatic C=O and the in-plane phenyl-ring bending mode ω (also the scissoring δ of the CH_2),

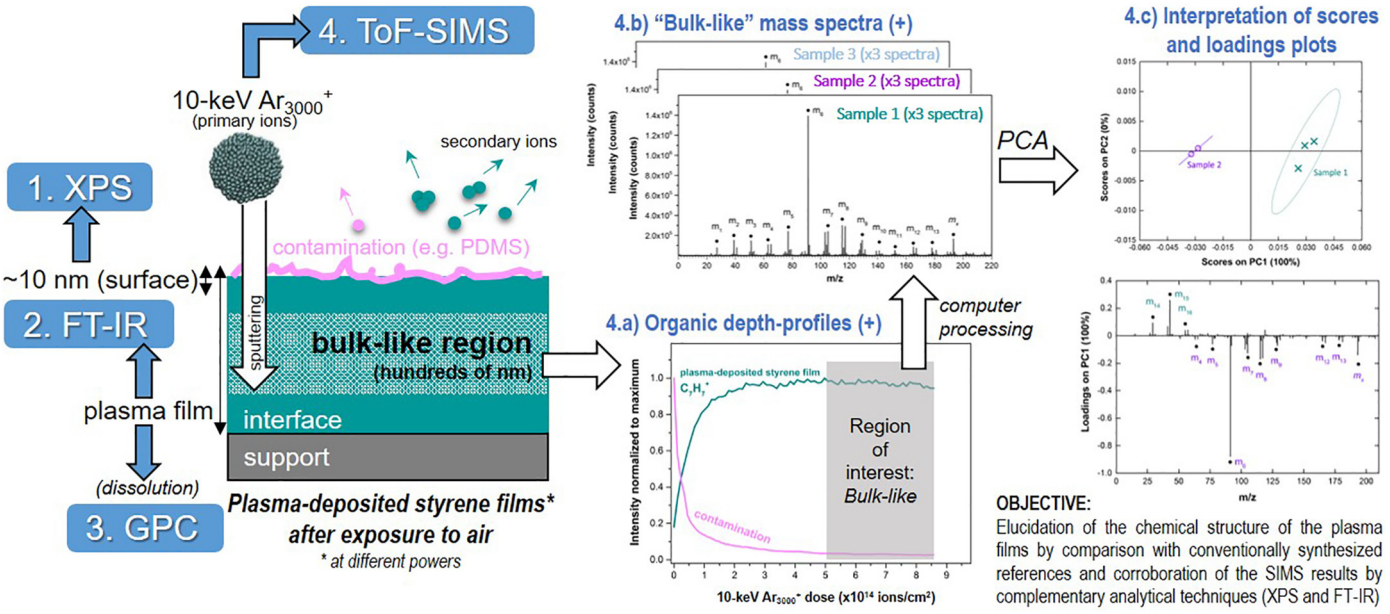

Scheme 1. Experimental approach applied for the ex-situ investigation of the chemical structure of the plasma-deposited styrene films.

Table 2
Elemental composition (determined by XPS and excluding hydrogen) and content (in %) of the functional groups derived from the decomposition of the C 1s peak for the PS reference sample (linear PS), and the pp-PS films synthesized at different plasma powers. **C**-(C,H) represents the sum of the aliphatic and aromatic components of the C 1s peak (**C**$_{aliph}$-(C,H) and **C**$_{arom}$-(C,H)) [39]. The last column lists the ratios of the O 1s peak to the **C**-O component of the C 1s peak (at 286.3 eV).

XPS peak	O 1s	C 1s						Si 2p
Assignment	–	Shake-up	O=**C**-O	**C**=O, O-**C**-O	**C**-O	**C**-(C,H)	C_{total}	–
Position (eV)	532.2	291.2	288.8	287.8	286.3	284.8	–	101.7

Sample									O 1s/**C**-O ratio
Linear PS	***0.7***	***6.6***	***0.0***	***0.0***	***1.5***	***91.2***	***99.3***	**–**	***0.5***
pp-PS/10W	7.2	4.8	0.3	2.5	8.5	76.7	92.8	–	0.8
pp-PS/20W	8.7	4.6	0.6	3.0	8.8	73.9	91.0	0.3	1.0
pp-PS/30W	7.7	4.1	0.7	3.2	9.1	75.2	92.3	–	0.8
pp-PS/40W	8.1	4.3	0.6	3.2	9.3	74.6	91.9	–	0.9
pp-PS/50W	8.4	4.1	0.3	2.0	9.1	76.2	91.6	–	0.9
pp-PS/60W	8.5	3.7	1.0	3.3	10.6	72.4	91.1	0.4	0.8
pp-PS/70W	9.2	3.6	0.8	4.0	11.1	70.8	90.4	0.4	0.8
pp-PS/80W	9.0	3.9	0.8	3.4	10.2	72.3	90.6	0.4	0.9

respectively. Going towards higher wavenumbers, specifically at 3027 and 2927 cm^{-1}, the aromatic CH and aliphatic CH_2 stretchings are observed. Oxidation is absent as demonstrated by the absence of the typical IR bands associated to O-based functional groups, such as the C=O asymmetrical vibration at 1716 cm^{-1} or the C-O asymmetrical vibration at 1268 cm^{-1}. Hence, the IR analysis of the polymer bulk confirms, after the XPS surface analysis, the adequacy of the linear PS as reference for this study. In addition, a comparison of the IR spectra of the linear PS and the styrene monomer (from NIST library) [43,44] was conducted in order to identify the main differences after polymerization. An important difference of the styrene spectrum consists in the absence of the aliphatic saturated CH stretching between 2850 and 2927 cm^{-1}, in addition to the presence of the vinyl (-CH=CH_2) stretching at 1640 cm^{-1} [45]. Furthermore, styrene and PS share absorption peaks related to the aromatic CH. The latter can occur in the same wavenumber range of aromatic CH or C=C (3010–3100 cm^{-1}, 1620–1680 cm^{-1} and 675–1000 cm^{-1}), so that the discrimination between unsaturation and aromaticity is difficult.

In Fig. 1.b, the IR spectra of two pp-PS films synthesized at different plasma powers are shown: pp-PS/30W, that represents the plasma-polymer deposited at low power, and pp-PS/80W, which constitutes the highest power in this investigation. These two infrared spectra (in transmission mode) are compared qualitatively with the one of the linear PS (cf. Fig. 1.a). At first glance, the two plasma-polymers are well synthesized. Indeed, one can observe the appearance of the aliphatic saturated CH stretchings between 2850 and 2927 cm^{-1}, which are absent in the styrene [45]. This is further confirmed by the absence of absorption bands characteristic of the vinyl group, such as the two strong bands at ~1000 and ~900 cm^{-1} [45]. Nevertheless, the presence of traces of free precursor molecules cannot be ruled out. In addition, the main finger-printing IR bands of the polystyrene are present in the IR spectra of the pp-PS deposits (listed in Table S1). However, some remarkable differences between the pp-PS and the conventionally polymerized PS exist [9], which are listed hereafter (Fig. 1):

A. The pp-PS appears oxidized in the bulk at all the plasma powers, as already shown by XPS at the surface. This is demonstrated by the presence of absorption peaks associated to O-based functionalities, such as the C=O and C-O stretching bands at 1716 and 1268 cm^{-1}, respectively. Also a broad band around 3400 cm^{-1}, associated to the stretching of -OH groups involved in H-bonds (very likely alcohol –OH groups or H_2O molecules trapped in the films) [46], is

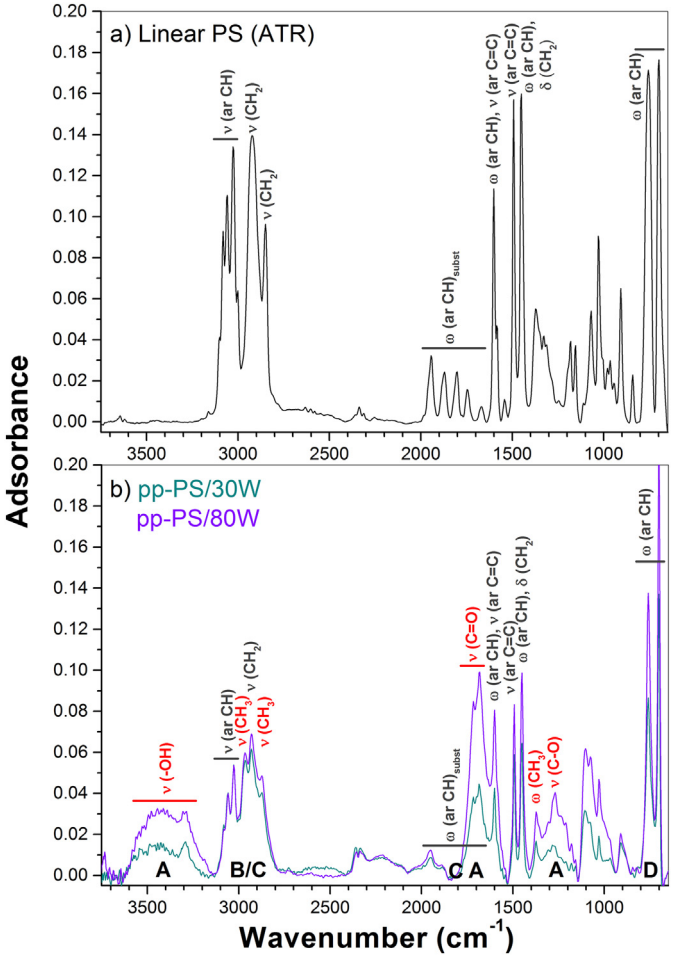

Fig. 1. a) IR-ATR spectrum of the commercial reference, linear PS. b) IR spectra acquired in transmission mode of two pp-PS films obtained at 30 W and 80 W, respectively. The main vibrational bands are identified in all the spectra. The appearance of new adsorption bands in the plasma-deposited films is indicated in color (red).

characteristic of these plasma polymers.

B. In the spectral range of the aliphatic saturated CH stretchings from 2960 to 2850 cm^{-1}, two new peaks appear in the pp-PS films: ν_{as} (aliphatic CH_3) at 2960 cm^{-1} and ν_s (aliphatic CH_3) at 2870 cm^{-1} [9]. This points out a significant presence of methyl groups totally unexpected for the conventional PS even at very low M_w (e.g. ~1000 g/mol) [47], where the -CH_3 constitutes only the chain ends of linear macromolecules. A plausible explanation of the -CH_3 presence in the pp-PS films, also observed for PS synthesized at lower pressures [3,12,48,49], would be the methyl-substitution or -CH_3 grafting (often indicated in the literature as branching) [9]. It is likely that CH_3· radicals are formed in the plasma-induced fragmentation of the precursor, and then they might recombine with radical sites on the aliphatic chains. Prohaska et al. hypothesized more specifically a structure for the pp-PS films similar to poly (α-methyl styrene) or poly (β-methyl styrene) with a certain degree of cross-linking (compare with the 3100–2850 cm^{-1} region of the IR spectrum of PAMS) [48,50]. Additionally, in the literature of pp-PS films synthesized near atmospheric pressure [9], the decrease of the ν_{as} (aliphatic CH_2) at 2927 cm^{-1} and the concomitant disappearance of the ν_s (aliphatic CH_2) at 2850 cm^{-1} are reported [9]. The authors hypothesized several factors, such as unsaturation, H abstraction, cross-linking, grafting of oxygen or -CH_3 on the aliphatic moieties of the polymer chain [9]. As already mentioned concerning the unsaturation, the alkene absorption peaks appear in the same wavenumber range as the aromatic ones, making its discrimination from the aromaticity problematic.

C. The pp-PS films show a decrease of the intensity of the vibrational bands of the aromatic CH above 3000 cm^{-1} compared to those of the aliphatic CH below 3000 cm^{-1}, accompanied by the decrease of the "five aromatic finger" bands between 1943 and 1666 cm^{-1}. This can be partly ascribed to the baseline correction. However, this observation can be mainly related to the partial destruction of the phenyl groups of the precursor in the plasma, in addition to a partial substitution of the aromatic rings as a consequence of cross-linking, for instance.

D. Prevalence of mono-substitution of the aryl groups as indicated by the $\omega_{out\text{-}of\text{-}plane}$ (aromatic CH) at 756 and 701 cm^{-1} in the pp-PS deposits [46]. However, the possibility of partial poly-substitution cannot be ruled out.

To some extent, an internal comparison of the pp-PS series was attempted. According to the work carried out by Prohaska et al. [48], the ratio of the peak heights of the ν (aromatic CH) at 3027 cm^{-1} to the ν_{as} (aliphatic CH_2) at 2927 cm^{-1} (2930 cm^{-1} in their study) (A3027/A2927) can be used as an indicator of the bulk aromaticity. Here, the following A3027/A2927 values of 0.957, 0.875 and 0.779 can be found for the linear PS (Fig. 1.a), pp-PS/30W and pp-PS/80W (Fig. 1.b). Therefore, the bulk aromaticity seems to decrease progressively with increasing plasma power as highlighted for the surface by XPS analysis. Prohaska et al. proposed also the indicator A2960/A2927 to describe the methyl-substitution in the pp-PS films, that is given by the ratio of the ν_{as} (aliphatic CH_3) at 2960 cm^{-1} to the ν_{as} (aliphatic CH_2) at 2927 cm^{-1} [48]. In this investigation, A2960/A2927 values are 0.91 and 0.88 for 30 W and 80 W respectively. This trend could be difficult to interpret without an adequate peak decomposition procedure.

3.3. GPC analysis

The chromatogram of the solution obtained from the pp-PS film deposited at 30 W (the thinnest deposit successfully analyzed in IR) is illustrated in Fig. S3. Two main weight distributions can be distinguished. The first molecular weight distribution below 1×10^3 g/mol is essentially constituted of oligomers ranging from 2 to 10 repeat units of PS and traces of the styrene precursor. The second main weight distribution above 1×10^6 g/mol is composed of long polymer chains (up to ~10,000 repeating units), linear or cross-linked. The higher population of oligomers compared to that of long polymer chains can be explained by the fact that smaller chains can be more easily desorbed from the polymer matrix. In addition, it can be presumed that the weight distribution above 1×10^6 g/mol does not represent the actual polymer network which, instead, remains on the support after prolonged immersion in the solvent (toluene). In the case of the pp-PS film synthesized at higher plasma power (60 W), the related chromatogram (not shown) looks very similar to the one reported in Fig. S3, except for a smaller (apparent) fraction of the polymer chains with $M_w > 1 \times 10^6$ g/mol. However, further comparisons of the two plasma films are not possible, since the relative percentage of dissolved polymer is unknown and probably very limited. In summary, GPC demonstrates the formation of a partially cross-linked polymer network (insoluble in the standard conditions applied for the dissolution of high M_w polystyrenes, probably also because of the high O content), in which an undetermined percentage of oligomers remains trapped.

3.4. Classical SIMS data treatment

Fig. 2 provides an overview of the bulk-like positive ion mass spectra of the sample set used for this SIMS study, i.e. the conventionally polymerized linear PS (reference) and the plasma films deposited at the lowest and highest powers, pp-PS/10W and pp-PS/80W. For the linear PS, the most intense ion fragments per each $C_xH_y^+$

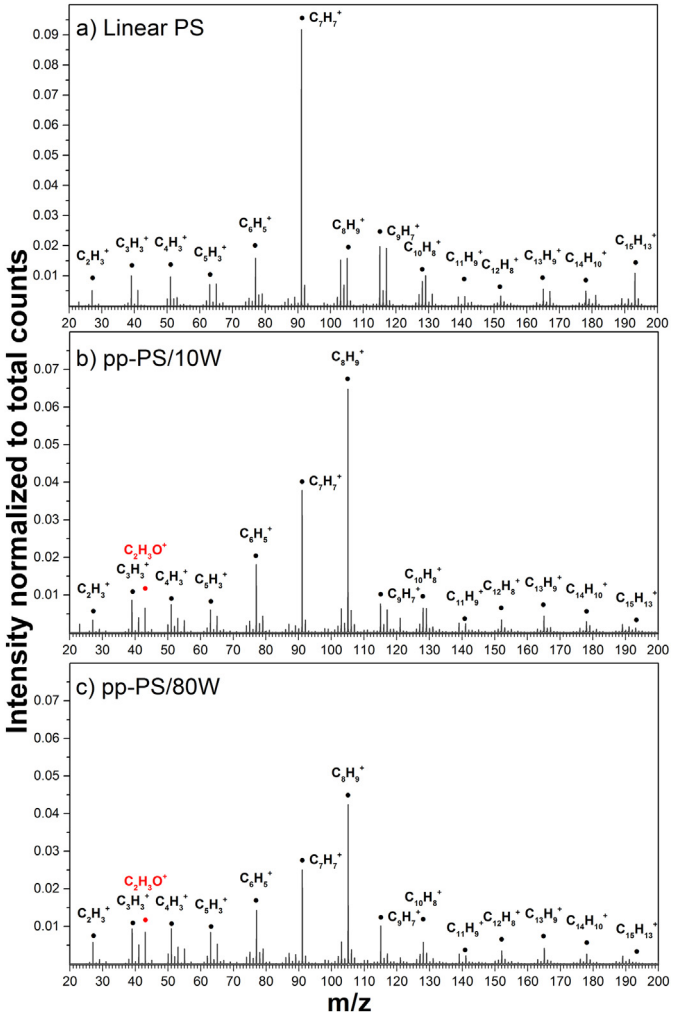

Fig. 2. Overview of the bulk-like positive ion mass spectra of the sample set used for this SIMS study. a) Conventionally polymerized linear PS used as reference; b,c) Two pp-PS films deposited at the lowest and highest plasma power. The most distinctive peaks of polystyrene are reported. For the plasma-polymers, the presence of oxidation is shown by the $C_2H_3O^+$ ion (in red).

(x = 2, 3, 4, 5, …, and y = 1, …, 2x + 1) series are at *m/z* 27, 39, 51, 63, 77, 91, 105, 115, 128, 141, 152, 165, 178 and 193. The most intense among these ions is the tropylium ($C_7H_7^+$) at *m/z* 91. This fragmentation pattern is in good agreement with the SIMS libraries, confirming the quality of the PS chosen as reference previously assessed by XPS and IR [51,52]. These characteristic secondary ions are very likely produced by re-arrangement reactions of species sputtered from the PS surface. However, the resulting ions are still PS structure-related fragments. Now, comparing the linear PS (Fig. 2.a) with the two pp-PS films (Fig. 2.b,c), the characteristic ions of PS are still traceable. The main difference between the conventionally polymerized and the plasma-synthesized PS concerns the inversed intensity ratio of the peaks 91^+ and 105^+, representing $C_7H_7^+$ and $C_8H_9^+$ respectively. The latter ion is postulated to be a methyl substitution of the tropylium ion [53]. In addition, the bulk-like positive ion mass spectra of the pp-PS deposits show the presence of O-uptake. However, further differences in the bulk-like mass spectra of the plasma films are very subtle. For this reason, a more quantitative approach for the analysis of the SIMS positive ion mass spectra should be applied. Several indicators of the structural properties of the coatings (e.g. aromaticity, branching and/or cross-linking contents) have been described in the SIMS literature, using generally ratios or normalized sums of secondary ion intensities. They were summarized in the feature paper published by Delcorte et al.

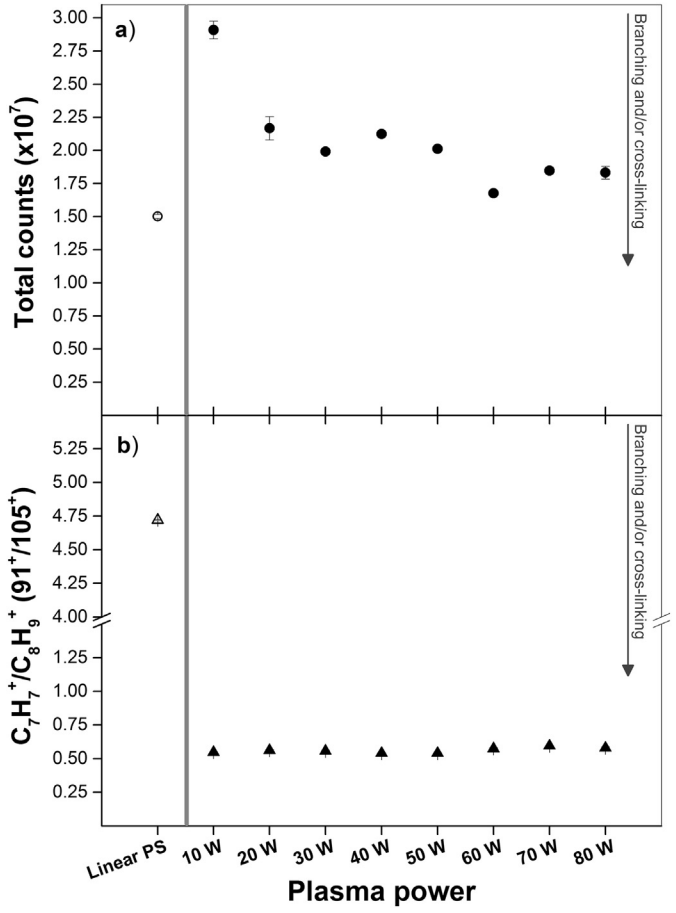

Fig. 3. Corrected total counts of the positive ion mass spectra reconstructed in the bulk region of the pp-PS films as a function of the plasma power (a), and the intensity ratio $C_7H_7^+/C_8H_9^+$ (b). For comparison purposes, the reference linear PS is reported on the left side of the graphs with open symbols.

[17]. For instance, Oran et al. looked at the total secondary ion yield or total counts in order to know the relative amount of the cross-linked character of a set of plasma-synthesized samples when varying the external plasma parameters [25,26]. The total secondary ion yield is expected to decrease as the cross-linked character increases [54]. However, the effects of cross-linking and branching are impossible to discern, so that differences in total counts are interpreted indiscriminately in terms of branching and/or cross-linking. The total counts of the positive ion mass spectra reconstructed in the bulk of the pp-PS films are reported in Fig. 3.a as a function of the plasma power.

Apparently, the branching and/or cross-linking increases with increasing power until reaching (roughly) the level of the reference linear PS at 80 W. However, any consideration based on this SIMS parameter is premature. Indeed, the total intensity of the mass spectra of the plasma deposits may be influenced by many unknown factors like the presence of oxidation, which increases with the power as pointed out by the XPS surface analyses. This could even determine an inversion between linear PS and pp-PS films, that could appear less branched and/or cross-linked (since the oxidation would enhance the probability of ionization of the latter samples). Moreover, other factors could influence the total counts, e.g. the ratio of oligomers to the highly polymerized pp-PS. Another indicator of the cross-linked character is proposed by Oran [25] and consists in the intensity ratio $C_7H_7^+/C_8H_9^+$ or $91^+/105^+$. Indeed, 91^+ and 105^+ are the most intense ions of the linear and plasma-polymerized PS, respectively. Thus, the first ion is attributed to a linear structure, whereas the second one to a more branched and/or cross-linked structure. Now, in Fig. 3.b, the linear PS

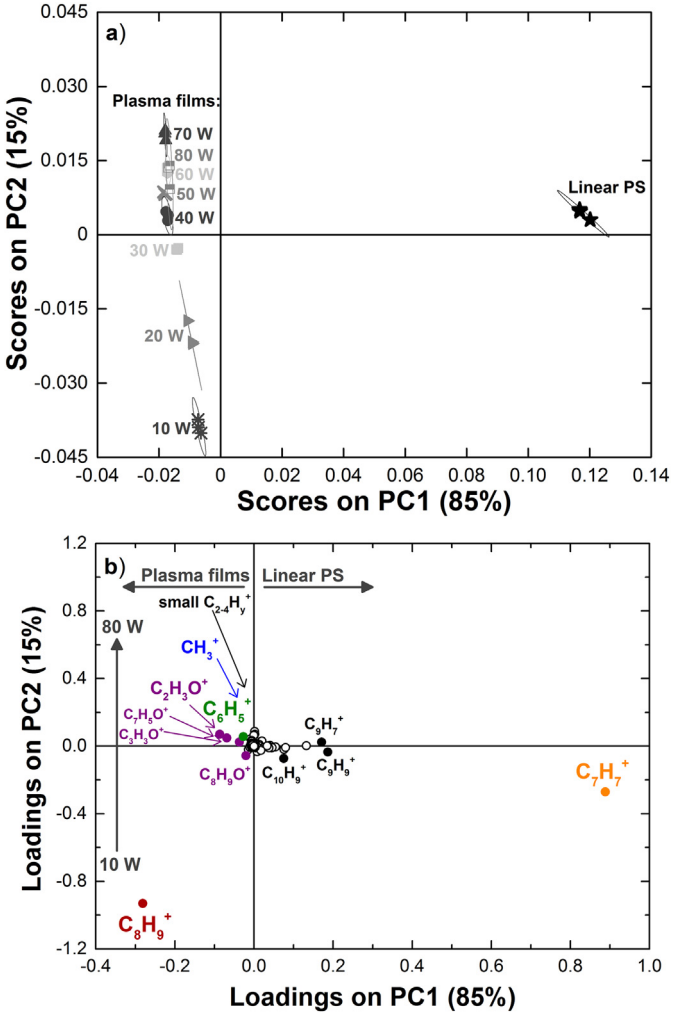

Fig. 4. PCA applied to the bulk-like positive ion mass spectra of the linear PS and the pp-PS films deposited at plasma powers ranging from 10 W to 80 W. a) PC2 versus PC1 scores plot, and b) PC2 versus PC1 loadings plot.

looks less branched and/or cross-linked than the plasma-polymer series. However, the ratio $C_7H_7^+/C_8H_9^+$ remains constant with increasing the plasma power, because of the simultaneous decrease of both ions. On the contrary, this intensity ratio is expected to decrease with increasing power because of a more pronounced increase of 105^+ on the decrease of 91^+. This situation demonstrates that the investigation of the structural features of the plasma-synthesized polymers, such as aromaticity, branching and/or cross-linking, cannot be based on the mere comparison of selected peak intensities, ratios or sums of peak intensities. For instance, the effect of the oxidation on the ionization probability of the above-mentioned secondary ions 91^+ and 105^+ is unknown. Hence, a more systematic and scientist-independent data treatment is required, that is multivariate analysis.

3.5. PCA applied to the bulk-like SIMS mass spectra of pp-PS

Fig. 4 reports the PCA results of the comparison between the pp-PS films and the reference linear PS. As shown in the scores plot (Fig. 4.a), PC1 discriminates the reference from the pp-PS, while PC2 points out the evolution of the chemical nature of the plasma films as a function of power. Loading thresholds of ± 0.01 and ± 0.025 have been set respectively for PC1 and PC2, in order to study the most influential ion fragments in the differentiation of the analyzed samples. In Fig. 4.b, PC1 positive loadings are associated to the linear PS. They correspond to the typical positive ion mass spectrum of PS, reflecting the aromatic structure of the polymer, where the most outstanding peak is the tropylium ion ($C_7H_7^+$ in orange). Among the PC1 negative loadings, representing the pp-PS films, dominate the protonated repeat unit of the PS, the ion $C_8H_9^+$ (in brown), in addition to the ion $C_6H_5^+$ (in green) and a series of O-containing fragments (in violet). A contribution to the ion intensities of $C_8H_9^+$ ($[p+H]^+$) and $C_6H_5^+$ ($[p\text{-}C_2H_3]^+$) could be due to the presence of traces of unreacted styrene precursor (p) in the deposited film, which cannot be ruled out by the IR, GPC and SIMS analyses. The ion $C_6H_5^+$ also represents the phenyl groups present in the polymer structure. Here, an important difference emerges between conventionally and plasma-polymerized PS: the inversed ratio of the ion intensities of 105^+ and 91^+. Concerning the oxidation, typical of the pp-PS films, the corresponding ions are either very small and linear, like $C_2H_3O^+$ and $C_3H_3O^+$, or bigger like $C_8H_9O^+$ and $C_9H_7O^+$, including an aromatic ring. This seems to indicate an O-grafting along the overall backbone of the polymer chains. It has already been proven by XPS that the oxidation increases with the power at the surface. Here, this is indicated by the decreasing trend of the PC1 negative scores going from 10 W to 80 W (Fig. 4.a). Lowering the loadings threshold, a third peculiar feature of the plasma-polymers can be observed: the increase of the aliphatic moieties in the polymer chains compared to the reference (small $C_{2\text{-}4}H_y^+$). This aliphatic fraction increases with increasing power, following the evolution of the O-uptake. Concerning PC2, loadings < 0 indicates which SIMS peaks decrease in relative intensity with increasing power. In that respect, PS-like fragments with $m/z \geq 91$ are associated to loadings < 0 (e.g. $C_8H_9^+$ and $C_7H_7^+$ in Fig. 4.b), as well as the dimer-related fragment $C_{16}H_{15}^+$ at m/z 207 ($[M\text{-}H]^+$, not shown). Thus, the relative intensity of these PS-like fragments decreases when the plasma power increases, better shown in Fig. 5.a. Furthermore, among the PC2 negative loadings, the oxidized ion $C_8H_9O^+$ is found, which follows the decreasing intensity trend of

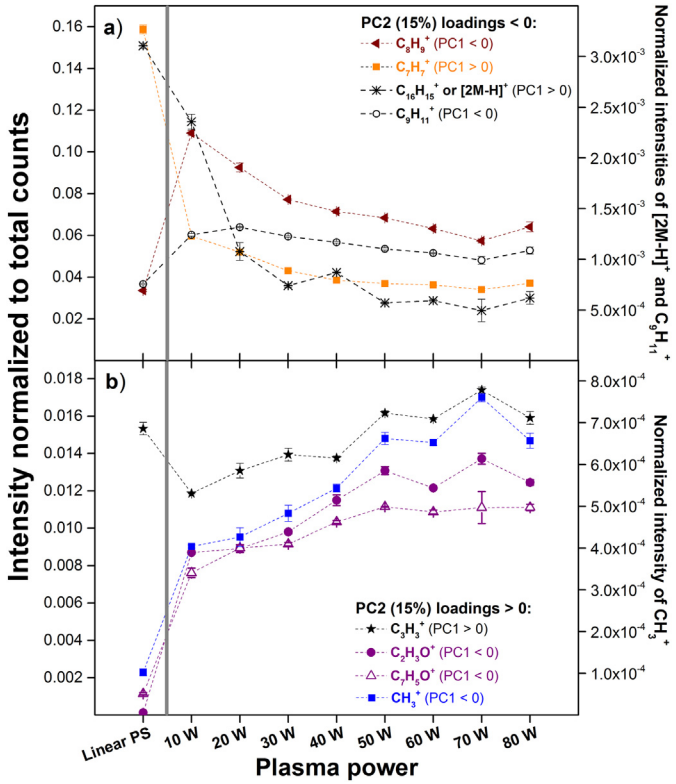

Fig. 5. Normalized intensities of some interesting secondary ions highlighted by the PCA study conducted on the pp-PS films synthesized at different plasma powers and the reference linear PS (reported separately on the left). PC2 negative loadings are associated to ion fragments that decrease in intensity with increasing plasma power, and vice versa.

$C_8H_9^+$. Conversely, loadings > 0 point out the SIMS peaks whose relative intensity increases with increasing plasma power. PC2 positive loadings are associated to smaller O-containing ions, such as $C_2H_3O^+$, $C_7H_5O^+$ and $C_3H_3O^+$, as well as smaller PS-like aliphatic fragments (e.g. $C_3H_3^+$, $C_4H_3^+$, $C_5H_3^+$, $C_2H_3^+$; small $C_{2\text{-}4}H_y^+$ in Fig. 4.b), and the aromatic ion $C_6H_5^+$. These ion intensities increase with increasing power applied to the discharge as depicted in Fig. 5.b. Then, in order to assess in SIMS the prevalence of mono-substitution of the aryl groups in the pp-PS deposits and the significant presence of methyl-substitution revealed by IR analysis, the evolution of the relative intensity of the ions $C_9H_{11}^+$ (119^+, PC1 and PC2 negative loadings) and CH_3^+ (15^+, PC1 negative loading, PC2 positive loading) was checked (cf. Fig. 5.a,b). $C_9H_{11}^+$ can be related to the alkyl-substitution of the phenyl rings. Indeed, if one looks at some poly (alkyl styrenes) mass spectra, such as those of the poly (2,4-dimethyl styrene) and the poly (2,5-dimethyl styrene) provided by the ION-TOF library, the peak at *m/z* 119 ($C_9H_{11}^+$) becomes the most intense one of the entire mass spectrum ($C_7H_7^+$: 25%, $C_9H_{11}^+$: 100%, and $C_7H_7^+$: 34%, $C_9H_{11}^+$: 100%, respectively) [52]. The $C_9H_{11}^+$ intensity of the plasma-polymers is slightly higher with respect to the linear PS, but very low compared to PS that has been cross-linked with divinylbenzene (DVB) (almost a factor 2; not shown). Instead, the ion CH_3^+ can be related to the presence of -CH_3 groups in the polymer matrix. The CH_3^+ intensity of pp-PS is much higher than for the linear PS and it increases with increasing power. The interpretation of these two different evolutions will be given in the Discussion section.

In order to explain the positive ion mass spectra of the pp-PS films dominated by $C_8H_9^+$, two commercial methyl-substituted PS have been selected as additional reference polymers according to the literature (Table 1) [48]: poly (α-methyl styrene) (PAMS) and poly (4-methyl styrene) (P4MS). In addition, to investigate the oxidized character of the pp-PS, as well as its cross-linked nature, poly (4-vinylphenol) (PVP) and cross-linked PS (XPS and IR characterization are reported in Table S2 and Fig. S4, respectively) are commercially available as reference materials. The positive ion mass spectra of these reference polymers normalized to the most intense peak are illustrated in Fig. S5.

The proposed PCA model constituted by the pp-PS films, linear PS, cross-linked PS, PAMS, P4MS and PVP is described by the first three principal components, representing together 97% of the total variance of the given dataset. The corresponding 3D scores plot is depicted in Fig. 6. PC2 versus PC1 scores plot shows that PAMS is the closest polymer to the pp-PS deposits, where a total variance of 87% is described. PVP and P4MS are substantially different from the investigated plasma samples, in addition to the linear PS. Instead, the cross-linked PS is more similar to the pp-PS deposits. PC3 (explaining the remaining 10% of variance) separates the plasma films (as well as the cross-linked PS) from PAMS and the other samples. A more detailed analysis of the PC1 loadings (not reported) indicates a different type of oxidation in the plasma-polymers compared to the PVP. Indeed, the positive ion mass spectra of PVP are mostly dominated by the ions $C_7H_7O^+$ at *m/z* 107 and $C_8H_9O^+$ at *m/z* 121, whereas the pp-PS films are mainly characterized by the ions $C_2H_3O^+$ at *m/z* 43 and $C_7H_5O^+$ at *m/z* 105. More generally, the intensity of the O-containing ions in the pp-PS deposits tends to that of the PVP only for small fragments like the $C_3H_3O^+$ at *m/z* 55. Thus, the oxygen in the plasma-polymers is bonded more likely to the backbone rather than directly to the phenyl ring like in the case of the PVP. However, it is hard to identify in SIMS the type of O-based functional groups present in the material, since different chemical functionalities produce common secondary ions [25]. Regarding PC2, the discrimination of the linear PS and the pp-PS is based on the partial loss of aromaticity in the latter indicated by the lower intensities of the ions 91^+, 115^+, 117^+ and 193^+. Concerning the separation in PC2 between the plasma films and the P4MS, it is fundamentally due to the higher ion intensities of 105^+ and 119^+ in the case of the methyl-substituted PS. Then, it is possible to rule out the massive presence of para-methyl substitution of the aryl groups in the

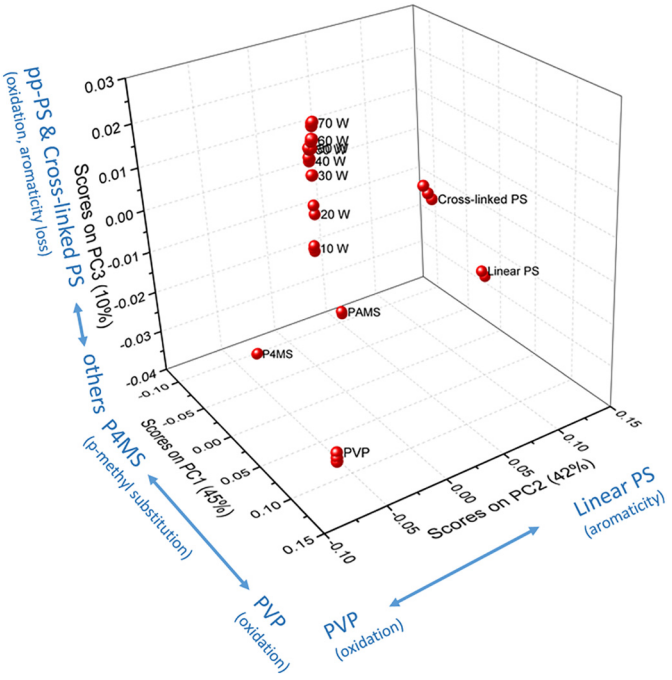

Fig. 6. 3D scores plot (explaining 97% of the overall variance) obtained from the PCA applied to the ToF-SIMS positive ion mass spectra of the pp-PS films synthesized at plasma powers ranging from 10 W to 80 W, the two commercial PS samples (linear and cross-linked), the two methyl-substituted PS (PAMS and P4MS), and the PVP. Three spectra have been acquired per sample.

plasma-polymer network. This is in rather good agreement with the FT-IR analysis of the plasma samples. Finally, the PC3 separation of the pp-PS and cross-linked PS from the other samples is explainable by the oxidation (see $C_2H_3O^+$), common to both polymers, and the more irregular structure of the plasma films (see the increase of the $C_6H_5^+$ intensity, linked to a partial loss of the aromaticity that will be discussed later). Indeed, the cross-linked PS is characterized by an increased ratio of the small aliphatic ($C_{1\text{–}4}$) (almost) saturated ions to the aromatic ions, as well as the increased intensity of the ion $C_9H_{11}^+$, when compared to the linear PS. Both features derive from the synthesis of polystyrene in presence of a cross-linking agent (DVB) [55]. Indeed, the cross-linking induces an increase of the ratio of the aliphatic to aromatic fractions in the polymer structure (this feature is somehow similar in the pp-PS), in addition to the introduction of di-substitution of the phenyl rings as demonstrated by the $C_9H_{11}^+$. The evolution of the chemical nature of the pp-PS films as a function of the power emerges in PC3 in terms of an increase of the oxidation and decrease of the aromatic content. A final PCA comparing only the pp-PS films with PAMS, identifies the main differences and similarities between the two polymers and as a function of the plasma power (not reported). pp-PS deposits appear oxidized and characterized by the presence of short aliphatic moieties in the polymer network as suggested by ions like $C_5H_3^+$ at *m/z* 63, as well as the presence of phenyl groups derived from $C_6H_5^+$. Both features tend to increase with increasing plasma power. It is worth noticing that those ion intensities are very close to PAMS as shown in Fig. S6.a. Conversely, other characteristic ion fragments of PAMS decrease in the pp-PS films with increasing power, such as 105^+ and 91^+. Their intensities in pp-PS films are comparable to PAMS at low power only (Fig. S6.b). Finally, peaks at higher m/z, such as 119^+ (representing the $[M + H]^+$ of PAMS), 143^+, 128^+, 207^+, 115^+ are mostly characteristic of PAMS. In Fig. S6.b, a scale break is required to show the evolution of the much less intense 119^+ in the plasma series.

In conclusion, these last two PCA seem to suggest that, in the submonomer region, the mass spectra of pp-PS and PAMS are more similar than PS, linear and cross-linked, even if the presence of oxidation

remains a distinctive chemical feature of the plasma-polymer. Only this *m/z* region is really suited for the comparison of conventionally synthesized polymers with the plasma counterparts, the latter being deprived of repeat unit. This investigation permits also to exclude the prevalence of para-substitution of the aromatic rings by methyl and/or hydroxyl groups in the plasma films or due to conventional cross-linking (induced by the addition of DVB, for instance), that would lead to a different fragmentation pattern, exclusively in terms of relative ion intensities. Thus, the methyl groups of the investigated plasma-polymerized PS are either bonded along the aliphatic backbone (rather than to the phenyl rings like in the case of P4MS), or constitute chain ends.

3.6. Sputter yield volume of pp-PS

The sputter yield volume Y (nm^3/PI) of the pp-PS films analyzed by SIMS was calculated in order to complement the information about the size distribution of the soluble fraction of the plasma deposits obtained by GPC (Section 3.3). Indeed, Y (defined as the sputtered volume in nm^3 per incident primary ion *PI* or argon cluster projectile Ar_n^+ in this study) is a function of the polymer molecular weight M_w. Fragmentation of the macromolecules upon ion bombardment and chain entanglement are the determining factors of the Y dependence on M_w for linear hydrocarbon polymers [56]. In Fig. 7, the pp-PS films as a function of the discharge power (black solid squares) are compared with PS standards for GPC of different M_w in terms of Y (the latter dataset was published in reference [57]). For both measurement series, the sputtering was performed using a 10-keV Ar_{3000}^+ ion beam, but different sputter currents were employed [57]. However, a recent work shows a negligible influence of the current on Y [58]. Fig. 7 shows a good agreement between the Y values of the reference linear PS, a polydisperse bulk polymer, and the PS standards with $M_w > 5 \times 10^4$ amu (considering an experimental error of ~10%). Indeed, Y is independent of M_w for high polymerization degrees [57]. The pp-PS synthesized at powers ≥30 W locate at the same level as the polydisperse PS. This confirms that the polymerization of the styrene precursor (average $M_w > 5 \times 10^4$ amu) has occurred in the plasma chamber as already indicated by the GPC results for the soluble fraction of pp-PS/30 W coating (M_w distribution > 1×10^6 amu shown in Fig. S3). The presence of O-based functionalities in these deposits might induce an enhancement of the sputter yield volume (O content of ~7–9% determined by XPS) compared to the reference PS [35]. However, the extent of the O-uptake effect on Y remains within the experimental error. In any case, the oxidation of the pp-PS films, that increases with increasing power, cannot explain the gap between 10 W and the other powers. Y at 10 W is unexpectly high (almost a factor of 2 compared to the average Y value of the remaining plasma-polymers). pp-PS/10 W can be assimilated to PS 2 k (composed by ~20 repeating units), strictly in terms of sputtered volume properties. This observation could be related to the presence of a much higher fraction of oligomers (and lower cross-linking content) in the plasma films obtained at 10 W. The presence of a considerable fraction of oligomers trapped in the plasma-polymer (cross-linked) network has been pointed out by the GPC analyses presented in Section 3.3. The higher fraction of oligomers at lower powers might also explain the much higher intensities of the dimer-related ion $[2M-H]^+$ at *m/z* 207 (as well as $[M + H]^+$ at *m/z* 105) and the $[3M-H]^+$ ion at 10 W and to a lesser extent at 20 W compared to rest of the plasma series (see Fig. S7).

4. Discussion

4.1. Ratio $91^+/105^+$ and cross-linking

The pp-PS films were compared with the conventionally polymerized counterpart (linear PS) by SIMS depth-profiling, looking at their bulk in order to avoid the influence of the surface contamination (demonstrated in XPS) and, more importantly, the post-oxidation. The

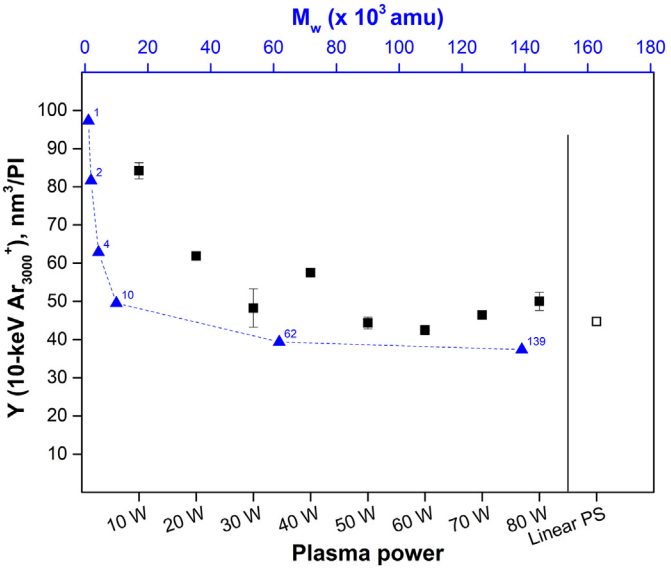

Fig. 7. Sputter yield volume (Y) of the pp-PS films as a function of the plasma power (black solid squares), the reference linear PS (black open square), and PS standards as a function of the M_w (blue curve). The values in blue type refer to the different M_w (x 10^3amu) of the polystyrene. The Y values of the plasma films result from the average of three independent SIMS measurements.

SIMS/PCA investigation reveals the inversed intensity ratio of the tropylium ion $C_7H_7^+$ (m/z = 91) and the postulated methyl-substituted tropylium ion $C_8H_9^+$ (m/z = 105). The tropylium ion is the most characteristic of both conventional polystyrenes (linear and cross-linked), whereas the methyl-substituted $C_8H_9^+$ becomes the most intense in the mass spectra of the whole plasma series (followed in intensity by $C_7H_7^+$ and $C_6H_5^+$ as illustrated in Figs. 2 and S5). Hence, the ion $C_8H_9^+$ represents a peculiar structural feature of the pp-PS deposited by plasma at sub-atmospheric pressure. This observation has already been reported for the pp-PS films deposited in DBD near atmospheric pressure[1] by Merche and co-workers using Ar or He as plasmagen gas [9]. Also the plasma polymerizations of the styrene precursor at low pressure carried out by Leggett and collaborators[2] in 1995 [20], and more recently by Oran[3] [25,26], showed the same spectral feature. Leggett and al. considered the $91^+/105^+$ ratio as an indicator of the cross-linked character of the plasma-deposited films (it decreases with increasing branching and/or cross-linking). Following the protocol proposed by Leggett et al. [20], Oran applied the $91^+/105^+$ intensity ratio to evaluate the increase of the cross-linked and/or branched content in the films synthesized from the styrene precursor by asymmetrical pulsed plasma as a function of the power and the duty cycle [25,26]. In this work the $91^+/105^+$ ratio decreases in the plasma films compared to the linear PS (thus the cross-linking and/or branching increases). However, conversely to what is expected, the ratio remains constant with increasing plasma power (see Fig. 3). This suggests a more complex situation where additional factors need to be taken into account, like for instance the oxidized character pointed out by the IR bulk characterization and quantified by XPS at the surface (from ~7% to ~9%). Indeed, the presence of oxidation can play an important role influencing the probability of ionization of secondary ions. This factor was not present in the plasma deposits prepared by Oran which, being synthesized at low pressure and then analyzed in-

[1] SSIMS spectra acquired on a PHI-Evans-TFS-4000 MMI (TRIFT 1) spectrometer with a source of 12-keV Ga^+ primary ions (600 pA).

[2] SSIMS spectra acquired with a quadrupole mass spectrometer by using 3.5-keV Xe^+ primary ions.

[3] A TOF.SIMS IV instrument was used with a 10-keV Cs^+ primary ion beam (0.75 pA).

situ, were devoid of oxygen [26].

4.2. Oxygen uptake

In this investigation, SIMS molecular depth-profiling demonstrates that relatively thick plasma-polymer films, like pp-PS/70 W (maximum thickness of ~8 μm, see Table 1), show constant signals of O-containing fragment ions in the inner layers (after a few tens of nm from the air/polymer interface) of the film down to the interface with the silicon substrate. This is consistent with the IR analyses (Fig. 1), which demonstrate a significant oxidation of the bulk of all the plasma films. Only in the outermost polymer layers, an increase of the O-based ions is observed in depth-profiles acquired a few hours after the plasma deposition. Moreover, from XPS (Table 2) and PCA (Fig. 4) the oxidation appears to increase with increasing power, probably as a consequence of the increase of the radicals formed in the polymer and those from the O_2 molecules. The O-uptake of films obtained from the styrene precursor plasma-polymerized in similar experimental conditions than those employed in this study was also detected by Merche and collaborators thanks to XPS, static-SIMS and FT-IR characterization [9]. In that work, the authors speculated that the O-uptake occurred during the plasma polymerization and/or it was due to post-polymerization oxidation in the air, since radical species remained trapped in the film after plasma deposition [42]. Optical emission spectroscopy (OES) of the Ar/DBD carried out by Merche shown Ar lines, together with impurities of nitrogen and small peaks of OH, but not O at 777 nm [9]. All these observations indicate that the O-uptake evidenced by the PCA study of the bulk-like region occurs in the reactor during the growth phase of the polymer deposit, rather than being the result of post-oxidation in the air.

4.3. Reduced aromaticity of the pp-PS films

pp-PS films show an increase of the ratio of the aliphatic to aromatic fractions compared to the linear PS. Thus, they are more assimilated to the cross-linked PS, especially at higher powers (Fig. 6). Moreover, the O-based functional groups seem to be grafted along the polymer aliphatic (un)saturated backbone, rather than to the phenyl rings. This can be partly confirmed by the PCA comparison with the fragmentation pattern of the poly (vinyl phenol) or PVP, where -OH groups are linked to the aromatic rings. XPS analysis elucidates that C-OH or alcohol groups are predominant at the surface of the pp-PS films, and that the oxidation increases of around 2% at the expense of the aromaticity (represented by the shake-up satellite) with increasing plasma power from 10 to 80 W (Table 2). This could suggest an oxidative functionalization of the phenyl rings with subsequent disruption of the aromaticity, as described by Potter et al. [42]. However, a concomitant fragmentation of the styrene molecules in the plasma medium, leading to the loss of aromatic rings [59], and the O-grafting to the aliphatic moieties of the polymer in growth cannot be excluded. OES conducted on the Ar/styrene discharge used in this study did not evidence the presence of any fragmentation products of the styrene molecule. These results are in rather good agreement with Merche's Ph.D. thesis [45]. This is supposed to be due to a strong dilution of the styrene in the more emissive Ar plasmagen gas. Emissive species of styrene are $C_4H_2{}^+$ (506.8 nm), CH· (431.4 nm), H_α and H_2 reported in the work of Chen and Yang [60], while Z. Li et al. individuate C_6H_6, CH, and C_2, among others [49]. Both cases deal with only styrene discharges. The decrease of the aromatic content in the plasma-polymers is confirmed in the bulk by IR characterization where, according to Prohaska [48] and Chen [3], it is also possible to determine that the aromaticity decreases as a function of the power (see the A3027/A2927 ratio). However, in IR the discrimination between aromaticity and unsaturation is problematic.

An important difference between cross-linked PS and pp-PS emerges through the $C_9H_{11}{}^+$ ion at *m/z* 119. Indeed, the alkyl-substitution (more precisely in position -para as elucidated by IR, see Fig. S4) of the cross-linked PS, due to the use of the cross-linking agent DVB, leads to an augmentation of small aliphatic saturated ions with respect to the linear PS, such as $CH_3{}^+$ or $C_2H_5{}^+$. Conversely, in the case of the pp-PS films, the increased intensity of $CH_3{}^+$ does not follow the $C_9H_{11}{}^+$ and $C_2H_5{}^+$. This is compatible with the prevalence of mono-substitution of the aryl groups found out in the IR analyses and a more unsaturated polymer backbone. This experimental evidence seems to indicate that the higher intensity of $CH_3{}^+$ with respect to the linear PS is related to the methyl-substitution of the plasma-polymer (i.e. branching) and/or the higher density of chain-ends, the latter being influenced by the cross-linking and the branching (impossible to discern). Concerning the methyl-substitution, it has already been reported in the literature for the case of the plasma-polymerized styrene since 1966 [61], but also for other polymer materials like the plasma-polymerized vinylferrocene [62] or the 2-vinylpyridine [63]. In the particular case of plasma-polymerized styrene at low pressure, Prohaska hypothesized a structure similar to the poly (α-methyl styrene) or poly (β-methyl styrene) on the basis of IR characterization [48]. Here, the comparison of the fragmentation pattern in the sub-monomer region of two methyl-substituted PS derivatives, i.e. PAMS and P4MS, seems to corroborate the fact that the -CH_3 groups are bonded to C_α, C_β, C_γ, and so on, but not to the phenyl rings. This is in agreement with the prevalence of mono-substitution observed in IR (Fig. 1). However, pp-PS films lack of repeat unit, being characterized by an irregular structure, cross-linked and branched. Thus, the high concentration of -CH_3 groups could be explained by the branching (point B of the IR analysis).

4.4. Effect of discharge power

The influence of the power applied to the plasma on the chemical structure of the pp-PS deposits was investigated in more details by SIMS/PCA. The evolution of the polymer structure in the given interval of powers show a saturation level towards 70–80 W (Fig. 4). Five "key" ions permit to summarize the structural variations of the pp-PS as a function of power (depicted in Fig. 8): $C_8H_9{}^+$ (105^+), $C_7H_7{}^+$ (91^+), $C_6H_5{}^+$ (77^+), $CH_3{}^+$ (15^+) (in decreasing order of *m/z* ratio) and $C_2H_3O^+$. Increasing the power, $C_8H_9{}^+$ and $C_7H_7{}^+$ decrease, in addition to the other PS-like fragment ions with m/z ≥ 91 (included $C_9H_{11}{}^+$ or 119^+, previously mentioned in the comparison with the cross-linked PS). Conversely, the aromatic ion $C_6H_5{}^+$ (related to the phenyl ring) at *m/z* 77 increases as well as a series of small aliphatic ions ($C_3H_3{}^+$, $C_4H_3{}^+$, $C_5H_3{}^+$, $C_2H_3{}^+$) and the $CH_3{}^+$. Small O-containing ions ($C_2H_3O^+$, $C_7H_5O^+$, $C_3H_3O^+$) increase with increasing power, while bigger oxidized ions like $C_8H_9O^+$ decrease. This mirrors the increase of the aliphatic fraction in the polymer matrix with the increase of power. Increasing the discharge power also affects the size distribution of the plasma polymer. GPC analyses carried out at 30 W and 60 W revealed the presence of oligomers (2–20 repeat units if compared to the PS standards), although the plasma films are well polymerized as demonstrated by the undissolved polymer matrix after several hours of immersion in the solvent and heating. This is also compatible with a high cross-linked character of the polymer deposited in the DBD at sub-atmospheric pressure. The significant presence of oligomers at 10 W is supported by the higher sputter yield volume (almost a factor of 2 with respect to 80 W, cf. Fig. 7). This higher presence of oligomers induces a higher density of -CH_3 chain ends, so that a significant contribution to the methyl-substitution observed in IR might come from the degree of polymerization. This factor, in combination with the -CH_3 grafting along the polymer backbone, might explain the inversed ratio $91^+/105^+$ that characterizes the plasma-deposited styrene films. Additionally, $C_8H_9{}^+$ (105^+) and $C_7H_7{}^+$ (91^+) decrease with power because of the more cross-linked polymer network. A higher cross-linked and/or branched content (established in XPS, IR, and SIMS), also leads to a relative increase of the emission probability of smaller fragment ions, like the aromatic $C_6H_5{}^+$ (77^+) and the aliphatic $CH_3{}^+$ (15^+).

In conclusion, all these experimental evidences point to an

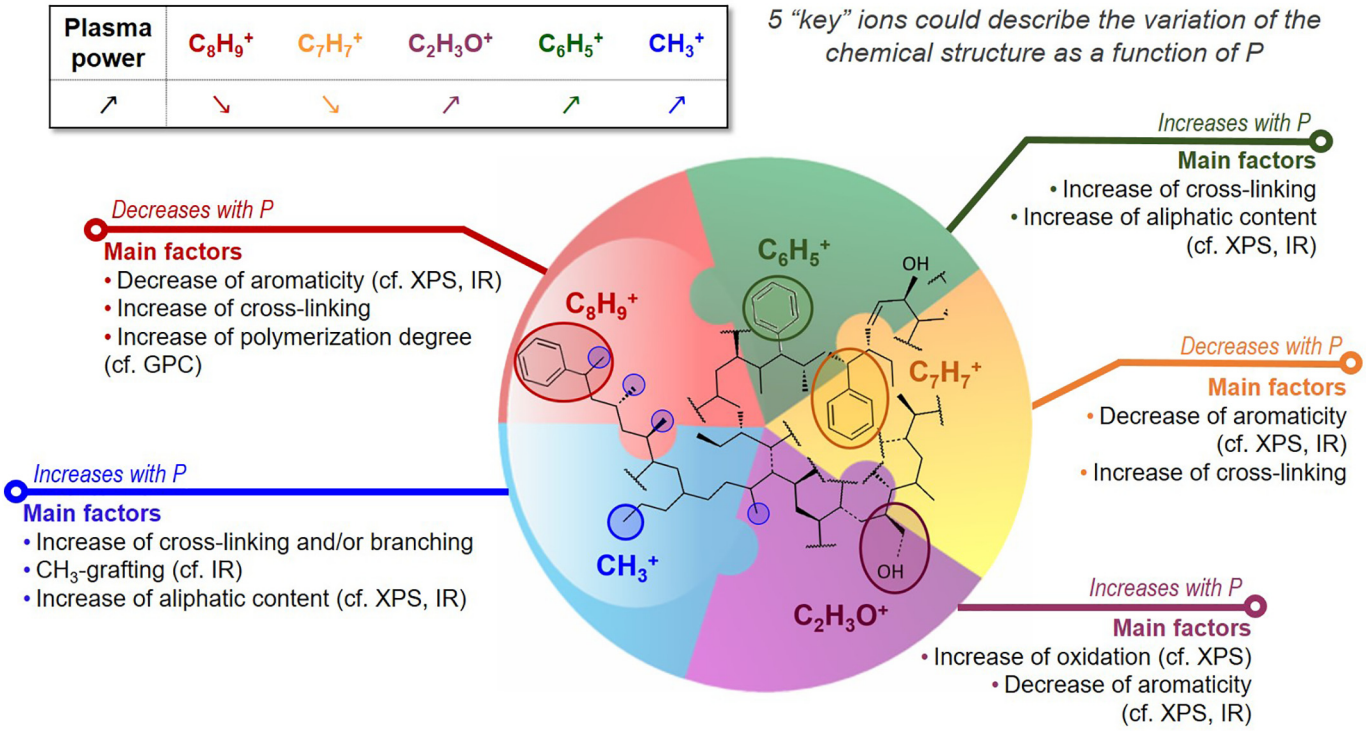

Fig. 8. Correlation between the evolution of the main spectral features of the pp-PS films (summarized by five "key" ions) and the variation of their chemical structure as a function of the plasma power (P), established by combined SIMS/PCA bulk characterization. Some of the determining factors pointed out by PCA are confirmed by other analytical techniques (bracketed), such as XPS (information at the surface), IR and GPC (information concerning the bulk).

enhancement of the fragmentation of the styrene precursor with increasing plasma power, and consequently a reduction of the aromaticity content in the resulting polymer deposits [25,64], accompanied by an increase of the branching/cross-linking and oxidized content and a diminution of the oligomer fraction trapped in the polymer structure.

5. Conclusion

The ex-situ characterization of plasma-deposited thin films by means of traditional analytical techniques such as IR, XPS, angle-resolved XPS and static-SIMS is usually very challenging because of the inevitable post-polymerization oxidation and surface contamination. For the first time, this study demonstrates that the chemical structure of plasma-synthesized polystyrene-like coatings can be elucidated after exposure to air, using ToF-SIMS depth-profiling with large Ar cluster ion beams in combination with principal component analysis. By reconstructing the mass spectra from a section of the depth-profile corresponding to the bulk of the film, post-polymerization oxidation triggered by long-lived radicals and other surface phenomena could be safely disregarded. In turn, this method provides a more accurate picture of the polymer film during the growth phase. In future works, the complementarity between SIMS and XPS should be strengthened by performing in-depth XPS characterization with a similar procedure (alternating Ar cluster ion beam etching with XPS analysis) in order to follow atomic concentrations and chemical shifts along the coating thickness.

In comparison with the other (bulk) analysis techniques used in this study such as FT-IR and GPC, beyond detailed molecular information, the specific interest of ToF-SIMS is that the information can be extracted very locally, with a typical resolution of a few nanometers in depth and one micrometer laterally (3D molecular imaging). Therefore, at variance with other techniques, films with a vertical variation of composition or molecular structure (e.g. difference between surface and bulk, near-substrate effects, stratified coatings, gradient layers) as well as laterally patterned coatings can also be precisely characterized. In addition to the traditional chemical and structural information provided by SIMS, we recently showed that information on local physical properties (Young's modulus, glass transition temperature, …) could also be retrieved by using the Ar cluster ion beam for analysis [65]. These methodological developments open the door to both chemical and physical characterization of complex plasma coatings in the three dimensions using secondary ion mass spectrometry.

Notes

Conflicts of interest: none.

Acknowledgements

The authors acknowledge the Belgian Science Policy Office for funding this work through the Interuniversity Attraction Pole (IAP Phase *VII*, convention: P7/34 'Physical Chemistry of Plasma Surface Interactions'). The authors also acknowledge the Belgian 'Fonds National de la Recherche Scientifique' (FNRS) for financial support to purchase the ToF-SIMS instrument. V. Cristaudo thanks Prof. Charles-Andrés Fustin, Prof. Jean-François Gohy and Dr. Olivier Bertrand for the GPC measurements performed at UCL, as well as Dr. Gaël De Leener for the GPC measurements conducted at ULB. Finally, V. Cristaudo thanks Sabine Bebelman for the FT-IR measurements and useful discussion.

Appendix A. Supplementary data

Supplementary data to this article can be found online at https://doi.org/10.1016/j.apsusc.2019.03.032.

References

[1] R. Denaro, P.A. Owens, A. Crawshaw, Glow discharge polymerization-styrene, Eur. Polym. J. 4 (1968) 93–106.

[2] L.F. Thompson, K.G. Mayhan, The plasma polymerization of vinyl monomers. II, a detailed study of the plasma polymerization of styrene, J. Appl. Polym. Sci. 16 (1972) 2317–2341.
[3] M. Chen, T. Yang, Z. Ma, Plasma polymerization of styrene with controlled particle energy, J. Polym. Sci. Pol. Chem. 36 (1998) 1265–1270.
[4] S. Swaraj, U. Oran, A. Lippitz, R.D. Schulze, J. Friedrich, W. Unger, Surface analysis of plasma-deposited polymers films, 2: analysis of post-plasma air reacted plasma polymerized styrene by X-ray photoelectron spectroscopy and X-ray absorption spectroscopy, Plasma Process. Polym. 1 (2004) 134–140.
[5] M. Haïdopoulos, J. Larrieu, M. Horgnies, L. Houssiau, J.J. Pireaux, A comparative study between inductively and capacitively coupled plasma deposited polystyrene films: chemical and morphological characterizations, Surf. Interface Anal. 38 (2006) 1266–1275.
[6] H.L. Luo, J. Sheng, Y.Z. Wan, Plasma polymerization of styrene with carbon dioxide under glow discharge conditions, Appl. Surf. Sci. 253 (2007) 5203–5207.
[7] S. Kurosawa, H. Harigae, H. Aizawa, J.W. Park, H. Suzuki, K. Terashima, Synthesis and characterization of microplasma-polymerized styrene and propargyl alcohol films, J. Photopolym. Sci. Tec. 18 (2005) 273–276.
[8] I. Topala, M. Asandulesa, D. Spridon, N. Dumitrascu, Hydrophobic coatings obtained in atmospheric pressure plasma, IEEE T. Plasma Sci. 37 (2009) 946–950.
[9] D. Merche, C. Poleunis, P. Bertrand, M. Sferrazza, F. Reniers, Synthesis of polystyrene thin films by means of an atmospheric-pressure plasma torch and a dielectric barrier discharge, IEEE T. Plasma Sci. 37 (2009) 951–960.
[10] D. Merche, N. Vandencasteele, F. Reniers, Atmospheric plasmas for thin film deposition: a critical review, Thin Solid Films 520 (2012) 4219–4236.
[11] M. Chen, T.C. Yang, Z. Ma, Investigation on RF styrene plasma by emission spectroscopy, IEEE T. Plasma Sci. 23 (1995) 151–155.
[12] I. Retzko, J.F. Friedrich, A. Lippitz, W.E.S. Unger, Chemical analysis of plasma-polymerized films: the application of X-ray photoelectron spectroscopy (XPS), X-ray absorption spectroscopy (NEXAFS) and Fourier transform infrared spectroscopy (FTIR), J. Electron Spectrosc. 121 (2001) 111–129.
[13] Z. Li, X. Gillon, L. Houssiau, J.J. Pireaux, Investigation in the synthesis process of plasma polymerisation: new polystyrene, Mater. Res. Innov. 19 (2015) S5-1117–S5-1123.
[14] F. Garbassi, E. Occhiello, F. Polato, A. Brown, Surface effect of flame treatments on polypropylene, J. Mater. Sci. 22 (1987) 1450–1456.
[15] E. Ochiello, M. Morra, G. Morini, F. Garbassi, P. Humphrey, Oxygen-plasma-treated polypropylene interfaces with air, water, and epoxy resins: part I. Air and water, J. Appl. Polym. Sci. 42 (1991) 551–559.
[16] Y. De Puydt, D. Léonard, P. Bertrand, Metallized Plastics 3: Fundamental and Applied Aspects, a Static SIMS Study of the Chemical Modifications Induced by Plasma and Flame Treatments at the Surface of Polyolefins. K. L. Mittal, Plenum Press, New York, 1992, p. 225.
[17] A. Delcorte, V. Cristaudo, M. Zarshenas, D. Merche, F. Reniers, P. Bertrand, Chemical analysis of plasma-treated organic surfaces and plasma polymers by secondary ion mass spectrometry, Plasma Process. Polym. 12 (2015) 905–918.
[18] W.J. Van Ooij, R.H. Brinkhuis, Interpretation of the fragmentation patterns in static SIMS analysis of polymers. Part I. Simple aliphatic hydrocarbons, Surf. Interface Anal. 11 (1988) 430–440.
[19] F.M. Petrat, D. Wolany, B.C. Schwede, L. Wiedmann, A. Benninghoven, Comparative in situ ToF-SIMS/XPS study of polystyrene modified by argon, oxygen and nitrogen plasmas, Surf. Interface Anal. 21 (1994) 402–406.
[20] G.J. Leggett, B.D. Ratner, J.C. Vickerman, Characterization of plasma-deposited styrene films by XPS and static SIMS, Surf. Interface Anal. 23 (1995) 22–28.
[21] A.J. Ward, R.D. Short, A tofsims and xps investigation of the structure of plasma polymers prepared from the methacrylate series of monomers: 2. The influence of the WF parameter on structural and functional group retention, Polymer. 36 (1995) 3439–3450.
[22] A.P. Ameen, R.D. Short, R.J. Ward, The formation of high surface concentrations of hydroxyl groups in the plasma polymerization of allyl alcohol, Polymer. 35 (1994) 4382–4391.
[23] S. Eufinger, W.J. van Ooij, K.D. Conners, DC-plasma polymerization of hexamethyldisiloxane. Part II. Surface and interface characterization of films deposited on stainless-steel substrates, Surf. Interface Anal. 24 (1996) 841–855.
[24] U. Oran, S. Swaraj, J.F. Friedrich, W.E.S. Unger, Surface analysis of plasma-deposited polymer films by Time of Flight Static Secondary Ion Mass Spectrometry (ToF-SSIMS) before and after exposure to ambient air, Surf. Coat. Tech. 200 (2005) 463–467.
[25] U. Oran, Surface Chemical Characterization of Plasma-chemically Deposited Polymer Films by Time of Flight Static Secondary Ion Mass Spectrometry. Ph.D. Thesis, Free University, Berlin, 2005.
[26] U. Oran, S. Swaraj, J.F. Friedrich, W.E.S. Unger, Surface analysis of plasma-deposited polymer films, 1, Plasma Process. Polym. 1 (2004) 123–133.
[27] D. Cossement, F. Renaux, D. Thiry, S. Ligot, R. Francq, R. Snyders, Chemical and microstructural characterizations of plasma polymer films by time-of-flight secondary ion mass spectrometry and principal component analysis, Appl. Surf. Sci. 355 (2015) 842–848.
[28] L. Denis, D. Cossement, T. Godfroid, F. Renaux, C. Bittencourt, R. Snyders, M. Hecq, Synthesis of allylamine plasma polymer films: correlation between plasma diagnostic and film characteristics, Plasma Process. Polym. 6 (2009) 199–208.
[29] L. Denis, F. Renaux, D. Cossement, C. Bittencourt, N. Tuccitto, A. Licciardello, M. Hecq, R. Snyders, Physico-chemical characterization of methyl isobutyrate-based plasma polymer films, Plasma Process. Polym. 8 (2011) 127–137.
[30] L. Denis, D. Thiry, D. Cossement, P. Gerbaux, F. Brusciotti, I. Van De Keere, V. Goossens, H. Terryn, M. Hecq, R. Snyders, Towards the understanding of plasma polymer film behaviour in ethanol: a multi-technique investigation, Prog. Org. Coat. 70 (2011) 134–141.
[31] S. Ligot, F. Renaux, L. Denis, D. Cossement, N. Nuns, P. Dubois, R. Snyders, Experimental study of the plasma polymerization of ethyl lactate, Plasma Process. Polym. 10 (2013) 999–1009.
[32] S. Ligot, E. Bousser, D. Cossement, J. Klemberg-Sapieha, P. Viville, P. Dubois, R. Snyders, Correlation between mechanical properties and cross-linking degree of ethyl lactate plasma polymer films, Plasma Process. Polym. 12 (2015) 508–518.
[33] D. Thiry, R. Francq, D. Cossement, M. Guillaume, J. Cornil, R. Snyders, A detailed description of the chemistry of thiol supporting plasma polymer films, Plasma Process. Polym. 11 (2014) 606–615.
[34] J. Hubert, C. Poleunis, A. Delcorte, P. Laha, J. Bossert, S. Lambeets, A. Ozkan, P. Bertrand, H. Terryn, F. Reniers, Plasma polymerization of C_4Cl_6 and $C_2H_2Cl_4$ at atmospheric pressure, Polymer. 54 (2013) 4085–4092.
[35] C.M. Mahoney, Cluster secondary ion mass spectrometry of polymers and related materials, Mass Spectrom. Rev. 29 (2010) 247–293.
[36] D.J. Graham, D.G. Castner, Multivariate analysis of ToF-SIMS data from multicomponent systems: why, when, and how, Biointerphases. 7 (2012).
[37] A.G. Shard, R. Havelund, M.P. Seah, S.J. Spencer, I.S. Gilmore, N. Winograd, D. Mayo, T. Miyayama, E. Niehuis, D. Rading, R. Moellers, Argon cluster ion beams for organic depth profiling: results from a VAMAS interlaboratory study, Anal. Chem. 84 (2012) 7865–7873.
[38] J.C. Vickerman, D. Briggs, ToF-SIMS: Materials Analysis by Mass Spectrometry, Second edition, IM Publications LLP and Surface Spectra Limited, Chichester, 2013, p. 656.
[39] G. Beamson, D. Briggs, High Resolution XPS of Organic Polymers: The Scienta ESCA 300 Database, John Wiley & Sons, Chichester, 1992.
[40] C.D. Wagner, L.E. Davis, M.V. Zeller, J.A. Taylor, R.H. Raymond, L.H. Gale, Empirical atomic sensitivity factors for quantitative analysis by electron spectroscopy for chemical analysis, Surf. Interface Anal. 3 (1981) 211–225.
[41] C. Poleunis, N. Médard, P. Bertrand, Additive quantification on polymer thin films by ToF-SIMS: aging sample effects, Appl. Surf. Sci. 231 (2004) 269–273.
[42] W. Potter, A.J. Ward, R.D. Short, The stability of plasma polymers: part I, a preliminary XPS study of the photostability of plasma polymerised styrene and methyl methacrylate, Polym. Degrad. Stabil. 43 (1994) 385–391.
[43] IR Spectrum of Styrene: NIST Chemistry Webbook, http://webbook.nist.gov/cgi/cbook.cgi?ID=C100425&Type=IR-SPEC&Index=2 , Accessed date: 21 May 2018.
[44] G. Varsányi, Assignments for Vibrational Spectra of 700 Benzene Derivatives, Hilger, London, 1974.
[45] D. Merche, Synthèse et caractérisation de couches de polystyrène et de polystyrène sulfoné obtenues par polymérisation-plasma à pression (sub)-atmosphérique. Ph.D. Thesis, Université Libre de Bruxelles, 2011.
[46] R.M. Silverstein, F.X. Webster, Spectrometric Identification of Organic Compounds, John Wiley & Sons, New York, 1996, p. 136.
[47] FT-IR Spectrum of Polystyrene (M_w = 1000 g/mol), https://www.sigmaaldrich.com/belgium-francais.html (accessed 5 May 2017).
[48] G.W. Prohaska, E.D. Johnson, J.F. Evans, Preparation and characterization of plasma-polymerized styrene thin films, J. Polym. Sci. Pol. Chem. 22 (1984) 2953–2972.
[49] Z. Li, X. Gillon, M. Diallo, L. Houssiau, J.-J. Pireaux, Plasma diagnostic and analysis for the styrene polymerization by low pressure inductively-coupled plasma, Proc. 19th Int. Symp. Plasma Chem, 2009, pp. 1–4.
[50] FT-IR Spectrum of Poly (Alpha-methyl Styrene) (M_w ~10000 g/mol), https://www.sigmaaldrich.com/belgium-francais.html (accessed 5 May 2017).
[51] J.G. Newman, B.A. Carlson, R.S. Michael, J.F. Moulder, T.A. Hohlt, Static SIMS Handbook of Polymer Analysis, Perkin-Elmer Corporation, Eden Prairie (MN), 1991, p. 26.
[52] B.C. Schwede, T. Heller, D. Rading, E. Niehuis, L. Wiedmann, A. Benninghoven, The Münster High Mass Resolution Static SIMS Library. ION-TOF: Münster, Print edition VI.3, Volume II, Polymers (1999).
[53] D. Kuck, Mass spectrometry of alkylbenzenes and related compounds. Part I. Gas-phase ion chemistry of alkylbenzene radical cations, Mass Spectrom. Rev. 9 (1990) 187–233.
[54] U. Oran, Surface Chemical Characterization of Plasma-chemically Deposited Polymer Films by Time of Flight Static Secondary Ion Mass Spectrometry. Ph.D. Thesis, Free University, Berlin, 2005, 40 and 53.
[55] C.H. Huck, G.K. Bonn, Poly (styrene-divinylbenzene) based media for liquid chromatography, Chem. Eng. Technol. 28 (2005) 1457–1472.
[56] A. Delcorte, M. Mathieu, Macromolecular sample sputtering by large Ar and CH_4 clusters: elucidating chain size and projectile effects with molecular dynamics, J. Phys. Chem. C 119 (2015) 25868–25879.
[57] V. Cristaudo, C. Poleunis, B. Czerwinski, A. Delcorte, Ar cluster sputtering of polymers: effects of cluster size and molecular weights, Surf. Interface Anal. 46 (2014) 79–82.
[58] V. Cristaudo, C. Poleunis, A. Delcorte, Effect of nanoconfinement on the sputter yield in ultrathin polymeric films: experiments and model, Appl. Surf. Sci. 444 (2018) 780–788.
[59] H. Yasuda, Plasma Polymerization, Academic Press, London, 1985.
[60] M. Chen, T.-C. Yang, Diagnostic analysis of styrene plasma polymerization, J. Polym. Sci. Pol. Chem. 37 (1999) 325–330.
[61] K. Jesch, J.E. Bloor, P.L. Kronick, Structure and physical properties of glow discharge polymers. I. Polymers from hydrocarbons, J. Polym. Sci. Pol. Chem. 4 (1966) 1487–1497.
[62] M.F. Dautartas, Studies of Plasma Polymerized Vinylferrocene Thin Films. Ph.D. Thesis, University of Minnesota, 1982.
[63] K.W. Bieg, D.K. Ottesen, Plasma Polymerization, M, Shen and A. T. Bell, Eds., ACs Symp. Ser. (1979) 108–128.
[64] I. Retzko, Pulsplasmapolymerisation von Acetylen, Ethylen, 1,3-Butadien Und Styrol. Ph.D. Thesis, Free University, Berlin, 2001.
[65] C. Poleunis, V. Cristaudo, A. Delcorte, Temperature dependence of Ar_n^+ cluster backscattering from polymer surfaces: a new method to determine the surface glass transition temperature, J. Am. Soc. Mass Spectr. 29 (2018) 4–7.